HHS Public Access

Author manuscript

Nature. Author manuscript; available in PMC 2013 November 10.

Published in final edited form as:

Nature. 2013 May 9; 497(7448): 211–216. doi:10.1038/nature12143.

Hypothalamic Programming of Systemic Aging Involving IKKβ/NF-κB and GnRH

Guo Zhang[1,2,3,4], **Juxue Li**[1,2,3,4], **Sudarshana Purkayastha**[1,2,3,4], **Yizhe Tang**[1,2,3,4], **Hai Zhang**[1,2,3,4], **Ye Yin**[1,2,3], **Bo Li**[1,2,3], **Gang Liu**[1,2,3], and **Dongsheng Cai**[1,2,3,*]

[1]Department of Molecular Pharmacology, Albert Einstein College of Medicine, Bronx, NY 10461

[2]Diabetes Research Center, Albert Einstein College of Medicine, Bronx, NY 10461

[3]Institute of Aging, Albert Einstein College of Medicine, Bronx, NY 10461

Summary

Aging is a result of gradual and overall functional deteriorations across the body; however, it is unknown if an individual tissue works to primarily mediate aging progress and lifespan control. Here we found that the hypothalamus is important for the development of whole-body aging in mice, and the underlying basis involves hypothalamic immunity mediated by IKKβ/NF-κB and related microglia-neuron immune crosstalk. Several interventional models were developed showing that aging retardation and lifespan extension are achieved in mice through preventing against aging-related hypothalamic or brain IKKβ/NF-κB activation. Mechanistic studies further revealed that IKKβ/NF-κB inhibits GnRH to mediate aging-related hypothalamic GnRH decline, and GnRH treatment amends aging-impaired neurogenesis and decelerates aging. In conclusion, the hypothalamus has a programmatic role in aging development via immune-neuroendocrine integration, and immune inhibition or GnRH restoration in the hypothalamus/brain represent two potential strategies for optimizing lifespan and combating aging-related health problems.

Keywords

Hypothalamus; aging; lifespan; longevity; NF-κ; IKKβ; GnRH; mice

Aging is characterized by gradual and overall loss of various physiological functions, leading to the end of lifespan. While the search for resolution of aging pathology is ongoing[1–6], research has shown that certain neurons can mediate environmental influences

[*]Address correspondence to: Dongsheng Cai, M.D., Ph.D., Department of Molecular Pharmacology, Albert Einstein College of Medicine, 1300 Morris Park Avenue, Bronx, New York 10461, Phone: 718-430-2426, Fax: 718-430-2433, dongsheng.cai@einstein.yu.edu.

[4]These authors equally contributed to this work.

Author contributions: DC conceived project and designed the study; GZ, JL, SP, YT, HZ, YY did experiments with assistance of BL and GL; All authors did data analyses and interpretations; DC organized experimentation and wrote the paper. Acknowledgements: The authors thank other Cai laboratory members for technical assistance, and thank L Farhana, D Stocco, L Eckhardt, T Ohshima, A Lin, and D Tantin for reagents. This study was supported by NIH grants R01 AG 031774, R01 DK078750, and ADA grant #1-12-BS-20 (all to D. Cai). DC is a recipient of Irma T. Hirschl Scholarship. The authors state that they have no competing financial interests.

on aging in *C. elegans* and *Drosophila*, and neural disruption of insulin/IGF-1 signaling was shown to increase lifespan in mice and worms[7–11]. In this study, we have focused on the hypothalamus, a key brain region that is crucial for the neuroendocrine interplay between the central nervous system and the periphery. We asked if the hypothalamus may have a fundamental role in aging development and lifespan control, in addition to its critical involvement in basic life-supporting functions such as growth, reproduction and metabolism. In tackling this bold question, we increasingly appreciated that an atypical collection of hypothalamic inflammatory changes can broadly and causally underlie the development of metabolic syndrome components including overweight, glucose intolerance and hypertension[12–15], and of note, all these disorders are often related to aging. Further, we have noted recent literature showing that microglia are involved in neurodegenerative diseases[16–24], which aligns with the appreciated connection between systemic immunity and aging[25, 26]. Herein, through targeting hypothalamic immunity/inflammation, we designed to test if the hypothalamus is fundamentally important for aging and lifespan control.

Aging-dependent hypothalamic NF-κB activation

In studying the potential role of the hypothalamus in aging, we developed a strategy of targeting hypothalamic immunity, and as shown in our recent work[12–15], infection-unrelated inflammatory changes in the mediobasal hypothalamus (MBH) underlies the development of various metabolic syndrome components, and the molecular basis is mediated critically by NF-κB and its upstream IκB kinase-β (IKKβ). Indeed, using NF-κB subunit RelA phosphorylation to report NF-κB activation, we observed that while hypothalamic NF-κB was barely active in young mice, it was activated in the hypothalamus of mice at middle-old ages, and the activities further increased when mice became older (Fig. 1a&b). Agreeing with this observation, mRNA levels of many cytokines and immune regulators increased in the hypothalamus of old mice compared to young group (data not shown). To directly visualize NF-κB activity in the MBH, we employed NF-κB reporter which induces GFP upon the binding of NF-κB to its transcriptional response element in a lentiviral vector (Fig. 1c). After in vitro assessment of this approach (suppl. Fig. 1a & b), we performed animal experiments by delivering this lentiviral NF-κB reporter into the MBH of mice at young, middle-old, and old ages. A prolonged recovery period was used to minimize the procedure-related non-specific effects on NF-κB. We found that GFP was negligible in the MBH of young mice (Fig. 1c), but was evident in the MBH of middle-old mice and became more profound in old mice (Fig. 1c&d), confirming that aging is associated with hypothalamic NF-κB activation. We also injected this lentiviral NF-κB reporter into various other brain regions, and comparatively, the MBH was most sensitive to aging-related NF-κB activation (suppl. Fig. 1c – e). Of interest, immunostaining with Neuronal marker NeuN revealed that NF-κB activation in neurons was relatively modest under middle-old aging, but became prominent when age further increased (Fig. 1c&d). Thus, aging development is characterized by chronic activation of NF-κB-directed innate immune pathway predominantly in the hypothalamus.

Pro- and anti-aging by hypothalamic IKKβ/NF-κB activation or inhibition

We then tested our hypothesized involvement of IKKβ/NF-κB in hypothalamic control of aging, and our experiments focused on the MBH. Using MBH-directed lentiviral gene delivery as we previously established[12, 13], we delivered dominant-negative IκBα (^{DN}IκBα) to inhibit NF-κB, and constitutively-active IKKβ (^{CA}IKKβ) to activate NF-κB in MBH neurons, and MBH delivery of irrelevant protein GFP in the same lentiviral system was used as the control (Fig. 2a, suppl. Fig. 2a). Middle-old C57BL/6 mice received bilateral MBH lentiviral injections; use of middle-old age helped eliminate developmental concerns, and indeed, aging retardation can be achieved through intervention starting at a middle-old age[27]. These mice with MBH delivery of ^{DN}IκBα, ^{CA}IKKβ and control GFP were named MBH-IκBα, MBH-IKKβ and MBH-Con mice, respectively, and all mice were maintained under pair feeding of a normal chow so that they had similar daily food intake. Our longitudinal follow-up revealed that MBH-Con mice displayed a typical pattern of lifespan (Fig. 2b), which indicated that our approach of MBH injection was technically suitable. Importantly, we found that lifespan significantly increased in MBH-IκBα mice but decreased in MBH-IKKβ mice compared to controls (Fig. 2b). In parallel with lifespan analysis, separate mice were generated to evaluate aging-related physiology and histology. We assessed cognition and muscle endurance of mice at ~6 months post gene delivery, at which hypothalamic NF-κB indeed remained over-activated in MBH-IKKβ mice but suppressed in MBH-IκBα mice (suppl. Fig. 2b). In cognitive test, we found that compared to controls, MBH-IκBα mice performed better but MBH-IKKβ mice performed worse (Fig. 2c), and indeed all these mice were technically eligible for the test (suppl. Fig. 2c). These mice were also subjected to grip test, showing that aging-related muscle weakness was attenuated in MBH-IκBα mice but worsened in MBH-IKKβ mice (Fig. 2d). Further, these mice were examined for a panel of histological biomarkers including muscle size, skin thickness, bone mass, and tail tendon collagen cross-linking. As shown in Fig. 2e–h, aging-related changes of these biomarkers were dampened in MBH-IκBα mice but exacerbated in MBH-IKKβ mice. Finally, given that these data were based on males, we further generated female mouse models, and results from females agreed with the observations in males (suppl. Fig. 3). In sum, the hypothalamus has a unique role in the development of systemic aging, and hypothalamic IKKβ/NF-κB represents a driving force in this process.

Hypothalamic microglia in aging development

To further understand aging-related hypothalamic immunity/inflammation, we profiled microglia in the hypothalamus. Using immunostaining, we found that numbers of microglial cells in the MBH increased in an age-dependent manner (Fig. 3a&b). TNF-α over-production (Fig. 3a&c) and NF-κB activation (suppl. Fig. 4) were both detected in these microglial cells, indicating that they were inflammatory. We noted that under early aging, NF-κB activation was already evident in hypothalamic microglia; however, this change was still modest in hypothalamic neurons (Fig. 1c&d). Also as observed, TNF-α over-production was mostly limited to hypothalamic microglia during early aging, but became prevalent across the MBH which affected other neural cells (such as neurons) in this region. We additionally measured hypothalamic *TNF-α* mRNA levels in mice of different ages, and data obtained (suppl. Fig. 5a) well correlated with cell counting of TNF-α immunostaining (Fig.

3c). It should be mentioned that TNF-α is a gene product of NF-κB and also acts to activate IKKβ/NF-κB. Overall, our data indicate that TNF-α is generated mainly by microglia during early aging, and the paracrine actions of this cytokine on neighboring cells can lead to aging-associated neuronal IKKβ/NF-κB activation. In the literature, TNF-α is known to be neurotoxic or neuroprotective[28–30], which may reflect the differential functions of soluble vs. transmembrane TNF-α[30]. In our aging model, soluble TNF-α seems to be involved in IKKβ/NF-κB-mediated microglia-neuron crosstalk which controls systemic aging.

Anti-aging effect by blocking IKKβ in hypothalamic microglia

Subsequently, we generated a mouse model with IKKβ knockout in the MBH microglia through bilaterally delivering microglia-specific (CD11b promoter-driven) lentiviral Cre into the MBH of IKKβ$^{lox/lox}$ mice, and control mice were IKKβ$^{lox/lox}$ mice injected with Cre-deficient lentiviruses. Our assessment confirmed that Cre was delivered specifically in Iba-1-expressing microglia, and majority of these cells in the MBH were induced with Cre (suppl. Fig. 5b). By profiling these IKKβ knockout mice and matched controls both of which were generated at a middle-old age, we observed that IKKβ ablation in microglia prevented against the increase of microglial cells over aging (Fig. 3d, suppl. Fig. 5c). Moreover, IKKβ ablation prevented aging from inducing TNF-α expression not only in microglia but in neighboring cells. Such aging-related hypothalamic microglia-neuron crosstalk via IKKβ/NF-κB led us to predict that microglia-specific IKKβ ablation might slow down aging. To test this prediction, we continued to use this IKKβ knockout mouse model generated at a middle-old age, maintained them till old ages, and assessed their aging manifestations. Following technical evaluation (suppl. Fig. 5d – f), we tested these mice using Morris Water Maze, and data showed that microglia-specific IKKβ ablation reduced aging-related cognitive decline (Fig. 3e – g). Furthermore, IKKβ ablation resulted in improvements in aging-related muscle weakness (Fig. 3h) and tail collagen cross-linking (Fig. 3i). Altogether, hypothalamic microglia can act via IKKβ/NF-κB to contribute to role of the hypothalamus in aging development.

Genetic longevity by suppressing brain IKKβ

We further resorted to a genetic model of brain-specific IKKβ knockout mice, N/IKKβ$^{lox/lox}$ mice which we generated by breeding Nestin-Cre with IKKβ$^{lox/lox}$ mice as we described previously[13]. Compared to littermate wildtype (WT) with matched IKKβ$^{lox/lox}$ background, these knockout mice were indeed developmentally indistinguishable in terms of brain size and gross morphology (suppl. Fig. 6). We also compared IKKβ$^{lox/lox}$ mice to additional types of controls, and confirmed that all these mice were similar across a spectrum of aging-related physiological and histological changes (suppl. Fig. 7). In this context, we profiled aging-related physiology and pathology in N/IKKβ$^{lox/lox}$ mice and littermate WT. At an old age, after technical assessment (suppl. Fig. 8a – c), we subjected mice to Morris Water Maze (MWM), and found that N/IKKβ$^{lox/lox}$ mice outperformed WT (Fig. 4a). This cognitive improvement was specific to aging, since young N/IKKβ$^{lox/lox}$ mice and WT performed similarly (suppl. Fig. 8d – h). Thus, although NF-κB appears to have a role in the development of hippocampal synaptic plasticity[31–33], the net effect from suppressing brain IKKβ/NF-κB under aging paradigm is cognitively beneficial. Using grip test, we further

found that compared to WT, N/IKKβ$^{lox/lox}$ mice had a reduced extent of aging-related muscle weakness (Fig. 4b). Also, as shown in Fig. 4c–h, N/IKKβ$^{lox/lox}$ mice were protected against aging-induced muscle and skin atrophy, bone loss, and collagen cross-linking. In addition to males, female N/IKKβ$^{lox/lox}$ mice were studied, and the findings were consistent (suppl. Fig. 9). Also importantly, we did lifespan analysis through following a cohort of male N/IKKβ$^{lox/lox}$ mice and littermate WT. As shown in Fig. 4i, WT had a typical pattern of median and maximal lifespan; in contrast, N/IKKβ$^{lox/lox}$ mice showed a pronounced phenotype of longevity, with median lifespan 23% longer ($P = 0.0002$) and maximal lifespan 20% longer ($p < 0.05$) than WT. We recognize that the longevity phenotype of this genetic model could be a result of IKKβ inhibition jointly in neurons and glia, since Nestin-Cre is known to target neural stem/progenitor cells and derived neurons and glia. To summarize, longevity in this genetic model significantly recapitulates aging retardation from hypothalamic IKKβ/NF-κB inhibition, and technologically, aging retardation can be achieved via IKKβ/NF-κB inhibition across the brain without evident side effects or compromised efficacy.

Aging-related hypothalamic GnRH decline induced by NF-κB

To better depict the hypothalamic control of aging, we focused on neuroendocrine pathways of the hypothalamus, and identified that IKKβ/NF-κB negatively regulated gonadotropin-releasing hormone (GnRH). The classical action of GnRH is to regulate sex hormones and reproduction, but it has yet to be studied regarding if GnRH is important for whole-body aging. We found that aging was associated with reduced hypothalamic *GnRH* mRNA, and this change was reversed by IKKβ/NF-κB inhibition but enhanced by IKKβ/NF-κB activation (Fig. 5a–c, suppl. Fig. 10a). Using GT1–7 cells, a cell line of GnRH neurons, we confirmed that GnRH release from these cells decreased upon IKKβ/NF-κB activation but increased by IKKβ/NF-κB inhibition (Fig. 5d). To study if NF-κB might inhibit *GnRH* gene, we introduced *GnRH* promoter-driven luciferase into GT1–7 cells, and simultaneously activated or inhibited IKKβ/NF-κB in these cells. Results showed that *GnRH* promoter activity reduced ~50% upon IKKβ/NF-κB activation but increased 4–5 folds by IKKβ/NF-κB inhibition (Fig. 5e&f). Moreover, IKKβ/NF-κB activation increased *c-Fos*, *c-Jun*, *PKCα* and *PKCδ* mRNA levels (Fig. 5g), and this finding was meaningful, because c-Fos/c-Jun overexpression and PKC activation were both able to inhibit *GnRH* promoter (Fig. 5h). Further, IKKβ/NF-κB's inhibition on *GnRH* promoter was attenuated by blocking c-Fos/c-Jun (Fig. 5i) or by suppressing PKC pathway (suppl. Fig. 10b). Altogether, c-Fos/c-Jun and PKC pathways can work together to mediate the inhibitory effect of IKKβ/NF-κB on GnRH (Fig. 5j), and in conjunction with relevant literature[34], transcriptional integration of NF-κB and c-Jun seems to account for down-regulation of GnRH in the hypothalamus.

GnRH treatment prevents aging-impaired neurogenesis

Based on the known role of GnRH in regulating sex hormones, GnRH changes in our mouse models might correlate with changes in sex hormones, and this prediction was proved (suppl. Fig. 10c & d). However, a sex hormone may not be a primary mediator for aging phenotypes in our models, since hypothalamic IKKβ/NF-κB is important for aging in both sexes. This context provoked us to hypothesize that GnRH works as a primary mediator

independently of a specific sex hormone. To explore if GnRH exerts intra-brain actions to affect aging, we delivered GnRH into hypothalamic third-ventricle of old mice, and examined aging-related changes in brain cell biology. A striking observation was that GnRH promoted adult neurogenesis despite aging. Using 7-day BrdU tracking to report neurogenesis[12], we found that aging is characterized by diminished neurogenesis particularly in the hypothalamus and the hippocampus; however, this defect was substantially reversed by GnRH treatment (Fig. 6a–c). 30-day BudU tracking also confirmed that BrdU-labeled cells in GnRH-treated mice significantly survived (Fig. 6d&e). Of note, these effects were seen in not only the hypothalamus but the hippocampus and other brain regions (data not shown), reflecting that GnRH travels within the brain to promote neurogenesis. Therefore, given the leadership role of the brain in controlling whole-body physiology, the brain-wide neurogenesis induced by hypothalamic GnRH may provide an explanation regarding how the hypothalamus, a very small structure in the brain, could control systemic aging.

GnRH therapy decelerates aging development

Finally, to study if GnRH could affect aging, we subjected old MBH-IKKβ mice and MBH-Con described in Fig. 2 to daily GnRH therapy for a prolonged period, and then examined their aging physiology and histology. As we were also interested in testing if GnRH could act peripherally to affect aging, we treated mice with GnRH via peripheral injections. Excitingly, GnRH treatment reduced the magnitude of aging histology in control mice and abrogated the pro-aging phenotype in MBH-IKKβ mice (Fig. 6f–h). Interestingly, despite the peripheral administration, GnRH led to an amelioration of aging-related cognitive decline (Fig. 6i, suppl. Fig. 11). Thus, prolonged elevation of systemic GnRH can cumulatively yield actions on the brain; despite the mechanism remains to be studied, some GnRH-responsive brain regions outside of the blood-brain barrier, such as the median eminence, subfornical organ and area postrema, can have access to peripheral delivered GnRH. These effects of GnRH were not specific to a sex, as similar outcomes were shown in male (Fig. 6f–i, suppl. Fig. 11) and females (suppl. Fig. 12). For comparison, we treated MBH-IκBα mice with GnRH, and it turned out that GnRH did not further enhance the anti-aging phenotype in MBH-IκBα mice (suppl. Fig. 13), suggesting that NF-κB inhibition and GnRH action may work in the same pathway to counteract aging. Clearly, future studies are still needed to detail the central and peripheral roles of GnRH in hypothalamic control of aging; regardless, the body of data in this work can lead to the conclusion that the hypothalamus can integrate NF-κB-directed immunity and GnRH-driven neuroendocrine system to program aging development.

Discussion

In this work, we conceived that the hypothalamus, which is known to have fundamental roles in growth, development, reproduction and metabolism, is also responsible for systemic aging and thus lifespan control. Excitingly, through activating or inhibiting immune pathway IKKβ/NF-κB in the hypothalamus of mice, we were able to accelerate or decelerate aging process, leading to shortened or increased lifespan. Thus, in line with the literature which appreciated the effects of the nervous system on lifespan[7–11], our findings provide a proof of

principle to the hypothesis that aging is a life event that is programmed by the hypothalamus. Indeed, brain change is an early aging manifestation[4], and we reasoned that some hypothalamic alterations may act to motivate aging of the rest parts in the body, and this outreaching role of the hypothalamus aligns with the fact that it is the neuroendocrine "headquarters" in the body. Along this line, we further revealed a direct link between IKKβ/NF-κB activation and GnRH decline, and also importantly, we discovered that GnRH induces adult neurogenesis broadly in the brain, and GnRH therapy can greatly amend aging disorders. Thus, while inhibition of GnRH by NF-κB may lead to the end of reproductive length – which seems necessary for species' quality, it initiates systemic aging at the same time. Question remains regarding how hypothalamic IKKβ/NF-κB is activated in this process; speculatively, as deduced from some recent studies about SIRTs and NF-κB[35, 36], age increase-induced epigenetic changes might be accountable, which calls for future investigations.

To summarize, our study using several mouse models demonstrates that the hypothalamus is important for systemic aging and lifespan control. This hypothalamic role is significantly mediated by IKKβ/NF-κB-directed hypothalamic innate immunity involving microglia-neuron crosstalk. The underlying basis includes integration between immunity and neuroendocrine of the hypothalamus, and immune inhibition and GnRH restoration in the hypothalamus or the brain represent two potential strategies for combating aging-related health problems.

Method Summary

All mice in this study were in C57BL/6 background, and IKKβ$^{lox/lox}$ and Nestin-Cre mice were described previously[13]. Physiological analyses included open field, visual platform test, Morris Water Maze, T-maze, and grip test. Skin and muscle histology, bone mass via X-ray micro-CT, and tail tendon breaking time were examined using standard methods in the literature. Lentiviral DNAs, virus production, MBH injection, immunostaining, Western blot, and qPCR were described in our recent research[13]. *GnRH* promoter was analyzed in GT1–7 cells transfected with *GnRH* promoter-driven luciferase plasmids. Lifespan analyses were performed as detailed in Methods. Statistics included ANOVA and appropriate *post hoc* analyses for comparisons involving more than two groups and two-tailed Student t test for comparisons involving only two groups. Data were presented as mean ± SEM. $P < 0.05$ was considered significant.

Methods

Mouse models and treatments

Nestin-Cre mice and IKKβ$^{lox/lox}$ mice were described in our previous publications[15–17, 37], and maintained on C57BL/6 strain for >15 generations. C57BL/6 mice were obtained from Jackson Laboratory or National Institute of Aging, NIH. All mice were kept under standard and infection-free housing, with 12 light/12 dark cycles and 4–5 mice per cage. Pathogen-free quality was ensured with quarterly serology, quarterly histopathologic exams and routine veterinarian monitoring, and bacteriological test was additionally included. All mice in this study were maintained on a normal chow from LabDiet (Cat# 5001, 4.07 Kcal/gram).

Animal GnRH therapy: mice were subcutaneously injected with GnRH (Sigma) at the dose of 2 ng per mouse on daily basis for a period of 5 – 8 weeks. The Institutional Animal Care and Use Committee at the Albert Einstein College of Medicine approved all the procedures. General physiology: Body weight and feeding: Body weight and food intake were measured regularly using a laboratory scale. Grip test: We performed grip test to measure muscle endurance using the method as similarly described in the literature[38, 39], except for a homemade square grid with small mesh size which allow mice to hang for longer time. Briefly, a mouse was lifted by tail and placed on a homemade square grid (1-cm mesh size). The grid was then inverted 12 inches over a soft pad, and the mouse was allowed to hang by paws for a maximum of 5 min. The time that the mouse was able to hang was recorded during 5-min test period.

Lentiviruses and MBH injection

Dual synapsin promoter-directed lentiviral vector was used to drive neuron-specific gene delivery as previously established[15–17, 37]. These lentiviral vectors contain the cDNA of ^{CA}IKKβ or ^{DN}IκBα driven by one synapsin promoter and cDNA of GFP controlled by another synapsin promoter. To create lentiviral NF-κB reporter vector, a target plasmid was constructed to have GFP open reading frame controlled by a DNA cassette containing 5 tandem repeats of NF-κB transcriptional response element (TRE), according to the approach established in the literature[40]. The lentiviruses were produced from HEK293T cells via co-transfecting a target plasmid with two package plasmids (VSVg and delta 8.9) using $CaCl_2$. Lentiviruses were purified through ultracentrifugation. Intra-MBH viral injections were performed as we previously established[15–17, 37]. Briefly, under an ultraprecise stereotactic instrument (resolution: 10 μm) (Kopf Instruments), lentiviruses were bilaterally injected at the coordinates of 1.5 mm posterior to the bregma, 5.8 mm below the skull, and 0.2 mm lateral to the midline.

Cognitive behavioral tests

All mice were tested for general health, sensorimotor reflexes and motor responses before onset of all behavioral testing. Mice were maintained on a 12-h light/dark schedule in an isolation unit located inside the behavioral testing room. An Anymaze video tracking system (Stoelting Co) equipped with a digital camera connected to a computer was used to videotape the whole course of animal activities in training and experimental sessions of behavioral tests. **Open Field test** – Locomotor activities were assessed using the open field test[1]. The open field arena consisted of a clear Plexiglas chamber that was 40 cm × 40 cm, with walls that were 35 cm high. The arena was placed in a brown box to reduce visual cues. Mice were placed in the arena and were allowed to explore for 5 min, and measured for distance and time traveled and mean speed. **Morris Water Maze (MWM) test** – The maze was filled with 22 – 23°C water that was made opaque with Crayola non-toxic paint and was located in the center of a small square room with numerous extra-maze cues (various black shapes on white background, a cabinet and an experimenter). The diameter of the maze was 90 cm and was divided into four quadrants (northwest, northeast, southwest and southeast). A circular platform with a diameter of 10 cm was placed 25 cm from the wall in the center of the northwest quadrant. *Visual Platform Test*: The test was performed on a single day. There were 6 trials with 30-min inter-trial intervals. In the test, a visible flag was placed on

the top of the platform to increase the visibility, and the platform was placed on a random location for each trial. A mouse was placed on water, at the same starting location for all trials, and was measured for latency, distance and mean speed traveled to the platform. *Hidden-Platform Training*: Mice were first required to swim to and sit on a circular visible platform at 0.5 cm above water level for 10 sec. If mice could not find the platform within 60 sec, they were gently guided to the platform using a glass stirring rod. Mice were then subjected to 5 consecutive days of training, consisting of 2 trials per entry location (entry locations were north, south, east, and west) for a total of 8 trials per day. The platform was made invisible by submerging it 1 cm below the surface of the water. Mice were expected to find the location of the invisible platform, and measured for latency to reach the platform, distance traveled to reach the platform, path efficiency, time spent in and distance traveled in each quadrant as well as total distance and mean swim speed. *Probe Trial*: On Day 6, mice were subjected to a single probe trial, in which the platform was removed and mice were allowed to swim for 60 sec. Mice were measured for the amount of time spent in all quadrants, distance and number of times that mice crossed the location of the former platform, and total distance and mean swim speed. **T-Maze** – Mice were tested for reward (1:1 water/full-fat sweetened condensed milk) (Nestle) on a forced-choice alternation test in a T-maze with an opaque floor and plastic sides. Mice first received food restriction to reduce body weight by 5~10%, and then a 4-day adaptation to the apparatus with the reward. Following that, mice were given 6 pairs of training per day for 12 days, and tests of every 2 days were designated as a trial block. On the first trial of each pair, a mouse was placed in the start arm, forced to choose one of two goal arms in the T (the other is blocked by a removable door), and received the reward at the end. The mouse was kept in this goal arm for 15 – 20 sec and subsequently returned by the experimenter to the start arm. The animal was then given a free choice between two goal arms, rewarded for choosing the 'novel' arm (the one which was not chosen in the first trial of the pair), but punished for choosing the other goal arm (the one which was chosen on the first trial of the pair) using a 20 sec-blocking without the reward. The location of the sample arm (left or right) was varied across trials so that mice received equal numbers of left and right presentations, and no more than two consecutive trials with the same sample location. Mice were tested in squads of 4 – 5 to minimize variations in inter-trial intervals, which was 5 – 10 min for all animals throughout 12-day training period.

Ex vivo analyses

Collagen cross-linking: The method of tail tendon breaking test was used to examine collagen cross-linking, as described[41]. Briefly, a collagen fiber was teased from a mid tail section of the lateral tail tendon and tied to a 2-gram weight. The fiber was suspended into a bath containing 7 M urea at 45°C. The fiber breaking time was determined in quadruplicate for each mouse. Tissue histology: Skeletal muscles (quadriceps) and dorsal skin were dissected from mice, fixed in 10% neutralized formalin at 4°C overnight, and embedded into paraffin. Paraffin sections were prepared at 5-μm thickness and subjected to haematoxylin-eosin staining. Images were collected using an Axioskop II light microscope (Zeiss) and analyzed using Image J. Bone volume fraction (BVF) measurement: We adopted the procedure established in the literature[42]. Briefly, the left intact femurs were removed and analyzed via LaTheta LCT-100A X-ray micro CT scanner (Aloka Inc.) through mouse

physiology core facility at Albert Einstein College of Medicine. The distal part of femur encompassing the cancellous bone was analyzed. The trabecular and cortical bone regions were outlined for each CT slice by the software of the scan system. BVF was calculated as the trabecular bone volume (BV) divided by total bone volume (TV). A calibration phantom was used for calibration of each scan.

Immunostaining, histology and Western blot

Mice under anesthesia were perfused with 4% PFA, and brains were removed, post-fixed in 4% PFA, and infiltrated in 20%-30% sucrose. Brain sections were made at 10-μm thickness via a cryostat, blocked with serum, penetrated with Triton-X 100, treated overnight at 4 degree with primary antibody, followed by reaction with fluorescence-conjugated secondary antibody (Jackson), and imaged under a con-focal microscope. For BrdU staining, sections were pre-treated with 1M HCl for 30 min at 37 °C, followed by 5-min treatment with 0.1M sodium borate (pH 8.5). Primary antibodies included rabbit anti-Iba-1 (Wako), rabbit anti-GFAP (Millipore), mouse anti-TNF-α (Abcam), mouse anti-NeuN (Millipore), and goat anti-Cre antibody (Santa Cruz). Nissl staining: Freshly isolated mice brains were fixed in 4% paraformaldehyde in PBS for overnight at 4 °C. The fixed whole brains were then subjected to cryo-sectioning coronally, and frozen sections were stained to detect Nissl body by using NovaUltra Nissl stain kit (IW-3007, IHCWORLD) according to the manufacturer's instruction. Cell counting in immunostaining: serial brain sections across the MBH were made at the thickness of single cell (10 μm), and every 5 sections were represented by one section with staining and cell counting. The numbers in representative sections were multiplied by 5 to indicate the total numbers within 5-section thickness. Western blotting: animal tissues were homogenized, and proteins were dissolved in a lysis buffer, and Western blots were conducted as previously described[3]. Proteins separated by SDS/PAGE were identified by immunoblotting with primary rabbit anti-pRelA, anti-RelA and anti-β-actin antibodies (Cell Signaling) and HRP-conjugated anti-rabbit secondary antibody (Pierce).

DNA vectors, Cell culture, and molecular/biochemical analysis

Promoter sequence of rat GnRH gene was PCR amplified (-1934 to +21) from a rat genomic DNA preparation, and subcloned into the pGL3-basic luciferase reporter vector (Promega) using standard cloning strategies. pcDNA expressing ^{CA}IKKβ or ^{DN}IκBα vs. control were previously described[1–3], or pcDNA expressing HA-RelA was provided by A. Lin. RelA shRNA and control (GFP) shRNA vectors were obtained from Addgene (# 22507, 22508, and 31848), as studied in the literature[43] (RelA shRNA: GCA-TGC-GAT-TCC-GCT-ATA-A, control shRNA: ACA-GCC-ACA-ACG-TCT-ATA-T). Expression plasmids for c-Jun or c-Fos were provided by D. Stocco. Vectors expressing c-Jun or c-Fos shRNA or scramble shRNA control were provided by L. Fahana (c-Jun shRNA: AGT-CAT-GAA-CCA-CGT-TAA-C; c-Fos shRNA: TCC-GAA-GAG-AAC-GGA-ATA-A; scramble shRNA: GTT-ATT-ACT-GTT-CGA-TCG-C). Phorbol 12-myristate 13-acetate (TPA) and Calphostin-C were from Sigma-Aldrich. TPA or Calphostin-C was dissolved in DMSO and applied in cell culture medium at a final concentration of 0.2 μM or 0.01 μM, respectively, and DMSO did not exceed 0.1% of cell culture medium. GT1–7 cells were previously described[3], and cultured in a standard humidified incubator at 37°C and 5% CO2 with DMEM cell culture medium supplemented with 10% FBS, 2 mM L-glutamine, and PenStrep (50 U/ml penicillin

G, 50 μg/ml streptomycin). Transfection of cultured cells with luciferase plasmids and expression plasmids was performed through Lipofectamine 2000 (Invitrogen). Dual Luciferase Reporter Assay (Promega) was performed according to the manufacturer's instruction, and co-transfection of pRL-TK vector expressing Renilla Luciferase was used to internally control firefly activity. Empty plasmids pGL3 and pcDNA3.1 were used as negative controls. RNA was extracted by TRIzol (Invitrogen) and analyzed via SYBR green real-time PCR (StepOnePlus real-time PCR system, Invitrogen). Testosterone and estradiol were measured using testosterone and estradiol EIA kits (Cayman Chemical). GnRH was measured using Luteinizing Hormone-Releasing Hormone EIA Kit (Phoenix Pharmaceuticals).

BrdU labeling study

Mice were pre-implanted with cannula in the third ventricle, and after ~3-week recovery, they were subjected to neurogenesis assay or survival/differentiation assays. Neurogenesis assay: mice were daily pre-injected with GnRH vs. vehicle at the dose of 1 ng per day through cannula for 3 days, subsequently a single icv injection of BrdU (Sigma) at the dose of 10 μg (defined as Day 0), and continued to receive daily icv injections of GnRH (1 ng/day) vs. vehicle for 7 days before they were sacrificed for brain sectioning. Survival/differentiation assay: mice pre-received daily icv injections of GnRH (1 ng per day) vs. vehicle for 3 days, then daily icv injections of BrdU (10 μg/day) together with daily icv injections of GnRH (1 ng/day) vs. vehicle for 7 days (last day was defined as Day 7), and followed by continued daily icv injections of GnRH (1 ng/day) vs. vehicle until Day 30 when mice were sacrificed for brain sectioning.

Statistical analyses

Kolmogorov-Smirnov test was used to determine parametric distribution of data. ANOVA and appropriate *post hoc* analyses were used for comparisons involving more than two groups. Two-tailed Student's t tests were used for comparisons involving only two groups. Lifespan analysis was performed using Kaplan-Meier Survival analysis; the mutant and control survivorship curves were compared in pairs and P values were obtained with log-rank test. Maximal lifespan of mice were statistically analyzed using Chi-Squared test according to the literature[44]. All data were presented as mean ± SEM. $P<0.05$ was considered significant.

Supplementary Material

Refer to Web version on PubMed Central for supplementary material.

Reference List

1. Miller RA. Genes against aging. J. Gerontol. A Biol. Sci. Med. Sci. 2012; 67:495–502. [PubMed: 22459617]
2. Mattson MP. Pathways towards and away from Alzheimer's disease. Nature. 2004; 430:631–639. [PubMed: 15295589]
3. Masoro EJ. Overview of caloric restriction and ageing. Mech. Ageing Dev. 2005; 126:913–922. [PubMed: 15885745]

4. Finch CE. Neurons, glia, and plasticity in normal brain aging. Adv. Gerontol. 2002; 10:35–39. [PubMed: 12577689]
5. Zitnik G, Martin GM. Age-related decline in neurogenesis: old cells or old environment? J. Neurosci. Res. 2002; 70:258–263. [PubMed: 12391584]
6. Martin GM. Epigenetic gambling and epigenetic drift as an antagonistic pleiotropic mechanism of aging. Aging Cell. 2009; 8:761–764. [PubMed: 19732045]
7. Bishop NA, Guarente L. Two neurons mediate diet-restriction-induced longevity in C. elegans. Nature. 2007; 447:545–549. [PubMed: 17538612]
8. Fridell YW, Sanchez-Blanco A, Silvia BA, Helfand SL. Targeted expression of the human uncoupling protein 2 (hUCP2) to adult neurons extends life span in the fly. Cell Metab. 2005; 1:145–152. [PubMed: 16054055]
9. Alcedo J, Kenyon C. Regulation of C. elegans longevity by specific gustatory and olfactory neurons. Neuron. 2004; 41:45–55. [PubMed: 14715134]
10. Wolkow CA, Kimura KD, Lee MS, Ruvkun G. Regulation of C. elegans life-span by insulinlike signaling in the nervous system. Science. 2000; 290:147–150. [PubMed: 11021802]
11. Taguchi A, Wartschow LM, White MF. Brain IRS2 signaling coordinates life span and nutrient homeostasis. Science. 2007; 317:369–372. [PubMed: 17641201]
12. Li J, Tang Y, Cai D. IKKbeta/NF-kappaB disrupts adult hypothalamic neural stem cells to mediate a neurodegenerative mechanism of dietary obesity and pre-diabetes. Nat. Cell Biol. 2012; 14:999–1012. [PubMed: 22940906]
13. Zhang X, et al. Hypothalamic IKKbeta/NF-kappaB and ER stress link overnutrition to energy imbalance and obesity. Cell. 2008; 135:61–73. [PubMed: 18854155]
14. Purkayastha S, et al. Neural dysregulation of peripheral insulin action and blood pressure by brain endoplasmic reticulum stress. Proc. Natl. Acad. Sci. U. S. A. 2011; 108:2939–2944. [PubMed: 21282643]
15. Purkayastha S, Zhang G, Cai D. Uncoupling the mechanisms of obesity and hypertension by targeting hypothalamic IKK-beta and NF-kappaB. Nat. Med. 2011; 17:883–887. [PubMed: 21642978]
16. Okun E, Griffioen KJ, Mattson MP. Toll-like receptor signaling in neural plasticity and disease. Trends Neurosci. 2011; 34:269–281. [PubMed: 21419501]
17. Glass CK, Saijo K, Winner B, Marchetto MC, Gage FH. Mechanisms underlying inflammation in neurodegeneration. Cell. 2010; 140:918–934. [PubMed: 20303880]
18. Saijo K, et al. A Nurr1/CoREST pathway in microglia and astrocytes protects dopaminergic neurons from inflammation-induced death. Cell. 2009; 137:47–59. [PubMed: 19345186]
19. Saijo K, Collier JG, Li AC, Katzenellenbogen JA, Glass CK. An ADIOL-ERbeta-CtBP transrepression pathway negatively regulates microglia-mediated inflammation. Cell. 2011; 145:584–595. [PubMed: 21565615]
20. Saijo K, Glass CK. Microglial cell origin and phenotypes in health and disease. Nat. Rev. Immunol. 2011; 11:775–787. [PubMed: 22025055]
21. Lucin KM, Wyss-Coray T. Immune activation in brain aging and neurodegeneration: too much or too little? Neuron. 2009; 64:110–122. [PubMed: 19840553]
22. Villeda S, Wyss-Coray T. Microglia--a wrench in the running wheel? Neuron. 2008; 59:527–529. [PubMed: 18760689]
23. Villeda SA, et al. The ageing systemic milieu negatively regulates neurogenesis and cognitive function. Nature. 2011; 477:90–94. [PubMed: 21886162]
24. Yoshiyama Y, et al. Synapse loss and microglial activation precede tangles in a P301S tauopathy mouse model. Neuron. 2007; 53:337–351. [PubMed: 17270732]
25. Adler AS, et al. Motif module map reveals enforcement of aging by continual NF-kappaB activity. Genes Dev. 2007; 21:3244–3257. [PubMed: 18055696]
26. Peng B, et al. Defective feedback regulation of NF-kappaB underlies Sjogren's syndrome in mice with mutated kappaB enhancers of the IkappaBalpha promoter. Proc. Natl. Acad. Sci. U. S. A. 2010; 107:15193–15198. [PubMed: 20696914]

27. Harrison DE, et al. Rapamycin fed late in life extends lifespan in genetically heterogeneous mice. Nature. 2009; 460:392–395. [PubMed: 19587680]
28. Barger SW, et al. Tumor necrosis factors alpha and beta protect neurons against amyloid beta-peptide toxicity: evidence for involvement of a kappa B-binding factor and attenuation of peroxide and Ca2+ accumulation. Proc. Natl. Acad. Sci. U. S. A. 1995; 92:9328–9332. [PubMed: 7568127]
29. Bruce AJ, et al. Altered neuronal and microglial responses to excitotoxic and ischemic brain injury in mice lacking TNF receptors. Nat. Med. 1996; 2:788–794. [PubMed: 8673925]
30. Taoufik E, et al. Transmembrane tumour necrosis factor is neuroprotective and regulates experimental autoimmune encephalomyelitis via neuronal nuclear factor-kappaB. Brain. 2011; 134:2722–2735. [PubMed: 21908876]
31. Kaltschmidt B, et al. NF-kappaB regulates spatial memory formation and synaptic plasticity through protein kinase A/CREB signaling. Mol. Cell Biol. 2006; 26:2936–2946. [PubMed: 16581769]
32. Meffert MK, Chang JM, Wiltgen BJ, Fanselow MS, Baltimore D. NF-kappa B functions in synaptic signaling and behavior. Nat. Neurosci. 2003; 6:1072–1078. [PubMed: 12947408]
33. O'Mahony A, et al. NF-kappaB/Rel regulates inhibitory and excitatory neuronal function and synaptic plasticity. Mol. Cell Biol. 2006; 26:7283–7298. [PubMed: 16980629]
34. Huang W, Ghisletti S, Perissi V, Rosenfeld MG, Glass CK. Transcriptional integration of TLR2 and TLR4 signaling at the NCoR derepression checkpoint. Mol. Cell. 2009; 35:48–57. [PubMed: 19595715]
35. Kawahara TL, et al. SIRT6 links histone H3 lysine 9 deacetylation to NF-kappaB-dependent gene expression and organismal life span. Cell. 2009; 136:62–74. [PubMed: 19135889]
36. Michishita E, et al. SIRT6 is a histone H3 lysine 9 deacetylase that modulates telomeric chromatin. Nature. 2008; 452:492–496. [PubMed: 18337721]

Supplementary Reference List

37. Meng Q, Cai D. Defective hypothalamic autophagy directs the central pathogenesis of obesity via the IkappaB kinase beta (IKKbeta)/NF-kappaB pathway. J. Biol. Chem. 2011; 286:32324–32332. [PubMed: 21784844]
38. Banks WA, et al. Effects of a growth hormone-releasing hormone antagonist on telomerase activity, oxidative stress, longevity, and aging in mice. Proc. Natl. Acad. Sci. U. S. A. 2010; 107:22272–22277. [PubMed: 21135231]
39. Tillerson JL, Miller GW. Grid performance test to measure behavioral impairment in the MPTP-treated-mouse model of parkinsonism. J. Neurosci. Methods. 2003; 123:189–200. [PubMed: 12606067]
40. Mueller JM, Pahl HL. Assaying NF-kappa B and AP-1 DNA-binding and transcriptional activity. Methods Mol. Biol. 2000; 99:205–216. [PubMed: 10909087]
41. Flurkey K, Papaconstantinou J, Miller RA, Harrison DE. Lifespan extension and delayed immune and collagen aging in mutant mice with defects in growth hormone production. Proc. Natl. Acad. Sci. U. S. A. 2001; 98:6736–6741. [PubMed: 11371619]
42. Ramanadham S, et al. Age-related changes in bone morphology are accelerated in group VIA phospholipase A2 (iPLA2beta)-null mice. Am. J. Pathol. 2008; 172:868–881. [PubMed: 18349124]
43. Meylan E, et al. Requirement for NF-kappaB signalling in a mouse model of lung adenocarcinoma. Nature. 2009; 462:104–107. [PubMed: 19847165]
44. Wang C, Li Q, Redden DT, Weindruch R, Allison DB. Statistical methods for testing effects on “maximum lifespan”. Mech. Ageing Dev. 2004; 125:629–632. [PubMed: 15491681]

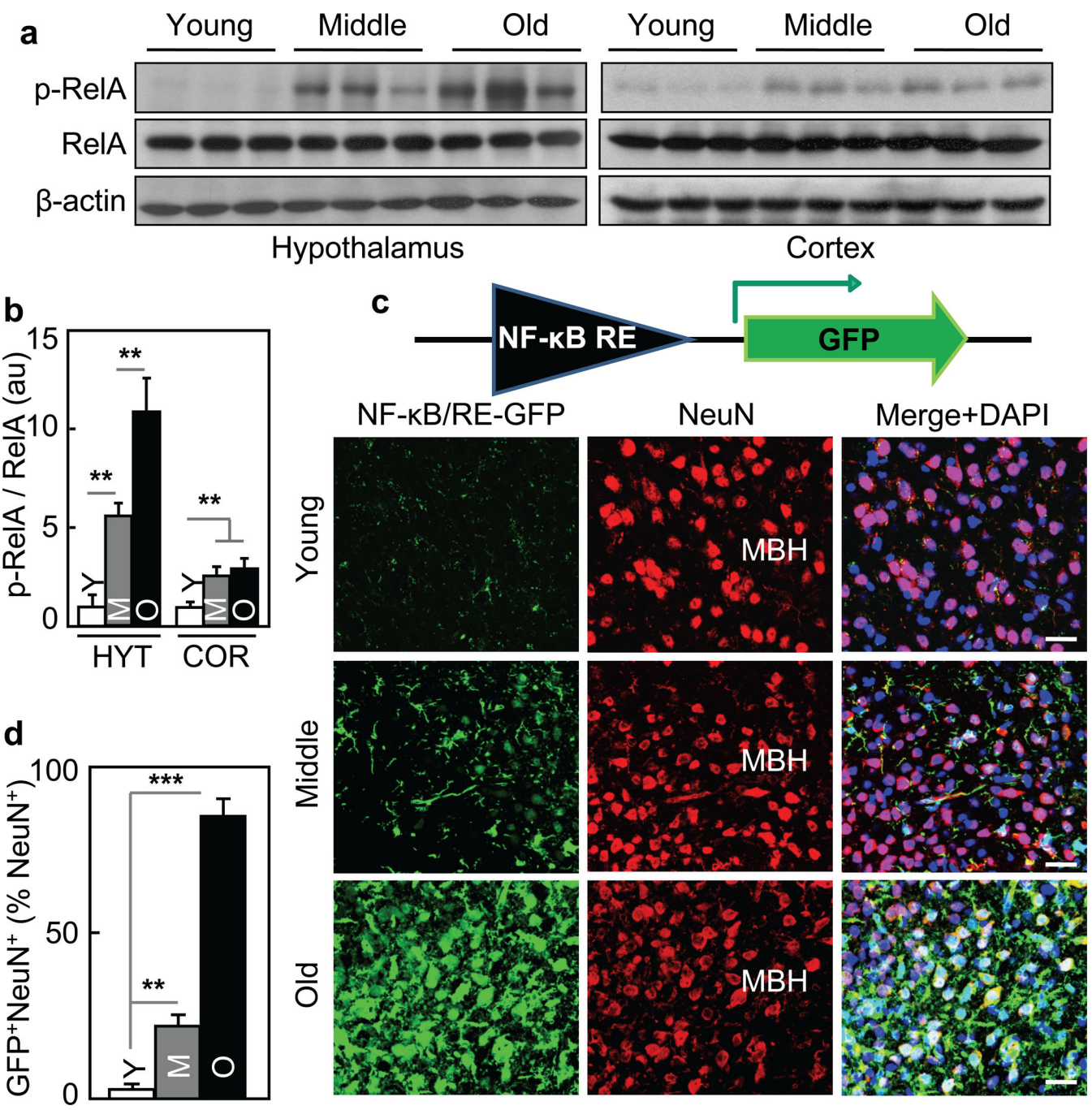

Figure 1. Aging-dependent hypothalamic NF-κB activation

57BL/6 mice (chow-fed males) were analyzed at young (3–4 months) age (Y), middle-old (11–13 months) age (M), and old (22–24 months) age (O). **a&b**. Hypothalami were analyzed via Western blots. **b:** Intensity of p-RelA normalized by RelA (au: arbitrary unit). **c&d**. Mice received MBH injections of lentiviral GFP controlled by NF-κB response element (NF-κB/RE), and following ~3-week recovery, brain sections were made to reveal GFP and NeuN stainining. DAPI staining shows entire cell populations. Bar = 25 μm. **d:** Percentages of cells co-expressing GFP and NeuN (GFP^+NeuN^+) among NeuN-expressing

cells **(**NeuN^{+}**)** in the MBH. **P < 0.01, ***P < 0.001; n = 6 (**b**) and 3 (**d**) per group. Error bars reflect mean ± SEM.

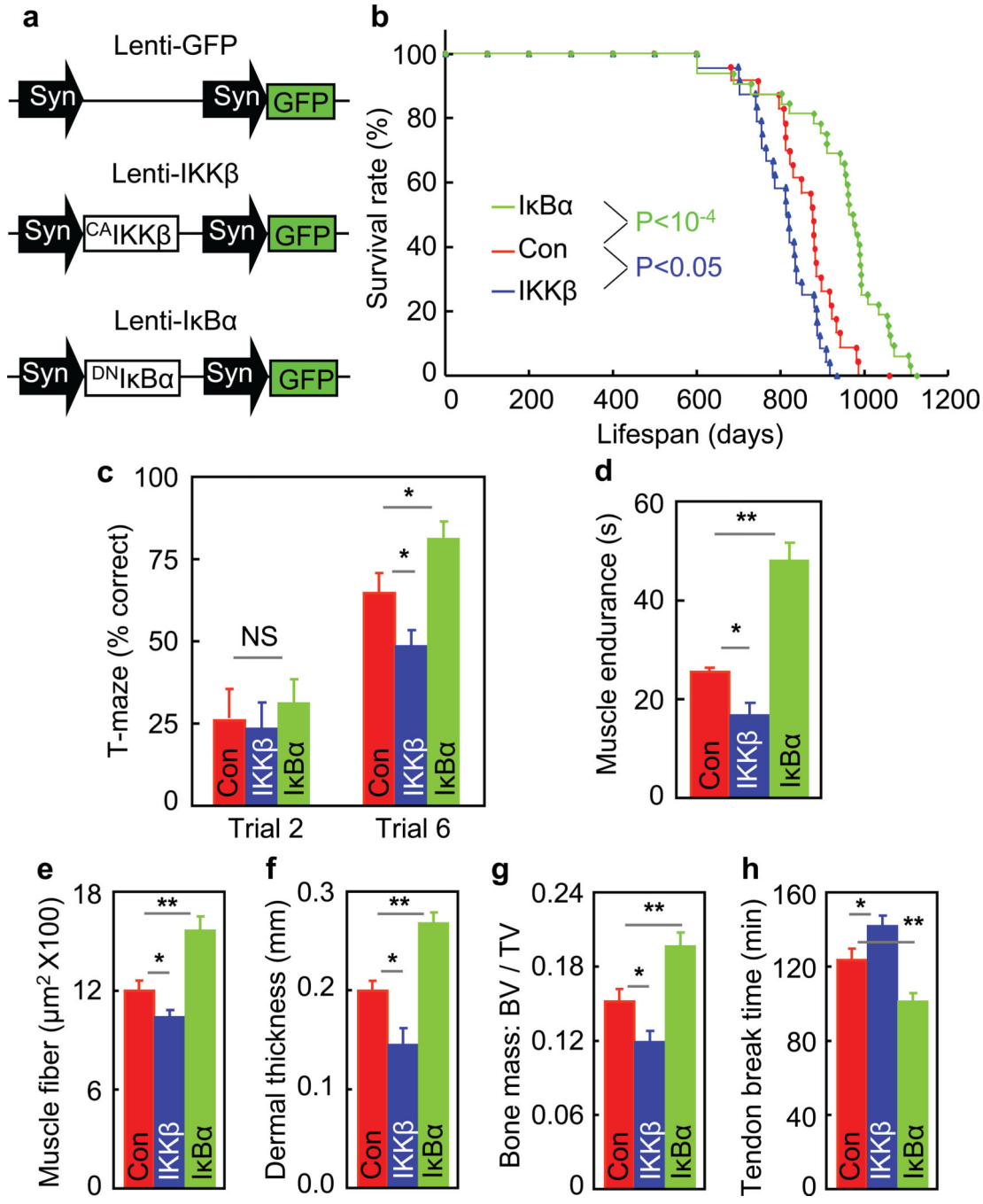

Figure 2. Aging manipulations by hypothalamic IKKβ/NF-κB

MBH-IKKβ, MBH-IκBα and MBH-Con mice were generated using ~18-month-old C57BL/6 mice (chow-fed males). **a**. Dual synapsin (Syn) promoter-directed lentiviral vectors. **b**. Lifespan of these mice (n = 23 – 31 mice per group). **c&d**. Mice at ~6 months post gene delivery were assessed for cognition via T-maze **(c)** and muscle endurance **(d). e–h:** Mice were scarified at 8~10 months post gene delivery for measuring muscle (quadriceps) fiber size (**e**), dermal thickness (**f**), bone mass (**g**), and tail tendon breaking time (**h**). *P < 0.05, **P < 0.01; MBH-Con: n = 23 **(b)**, 9 **(c)**, 6 **(d)**, 3 **(e&f)**, 4 **(g)**, and 7 **(h)**;

MBH-IKKβ: n = 24 **(b)**, 10 **(c)**, 6 **(d)**, 3 **(e&f)**, 4 **(g)**, and 5 **(h)**; MBH-IκBα: n = 31 **(b)**, 12 **(c)**, 7 **(d)**, 3 **(e&f)**, 6 **(g)**, and 8 **(h)**. Error bars reflect mean ± SEM.

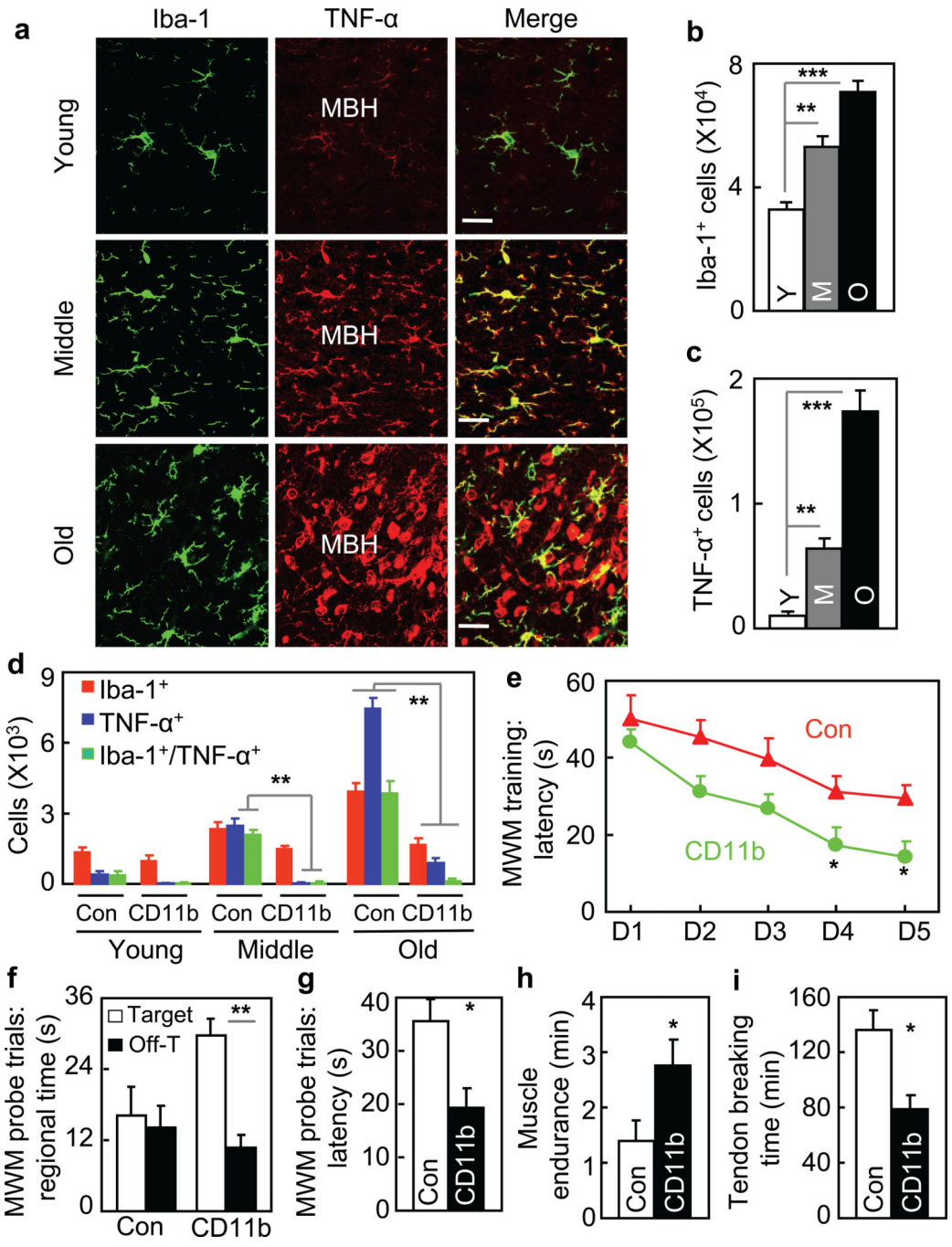

Figure 3. Role of hypothalamic microglia in aging

a–c Brain sections of young (Y), middle-old (M) and old (O) C57BL/6 mice were analyzed for hypothalamic microglia. **a:** Representative images of immunostaining. Bar = 25 μm. **b&c:** Numbers of cells expressing Iba-1 (Iba-1$^+$) **(b)** or TNF-α (TNF-α$^+$) **(c)** in the arcuate nucleus. **d**. Middle-old IKKβ$^{lox/lox}$ mice received bilateral MBH injections of lentiviral CD11b promoter-driven Cre (CD11b) vs. control (Con). At 1 month vs. 8 months post injection, brain sections were made for Iba-1 and TNF-α staining (images in suppl. Fig. 4c). Mice generated at a young age provided normal references. Data show numbers of cells

immunoreactive for Iba-1, TNF-α or both in the arcuate nucleus. **e–i**. Mice described in Fig. 3e were generated at a middle-old age and assessed at old ages for cognition **(e–g)**, muscle endurance **(h)**, and tail tendon breaking time **(i)**. MWM data included time in target vs. a representative off-target (Off-T) quadrant in probe trials. *P < 0.05, **P < 0.01, ***P < 0.001; n = 4 **(b&c)** and 3 **(d)** per group; Con: n = 6 **(e–g, i)** and 9 **(h)**; CD11b: n = 5 **(e–g)** and 6 **(h&i)**. Error bars reflect mean ± SEM.

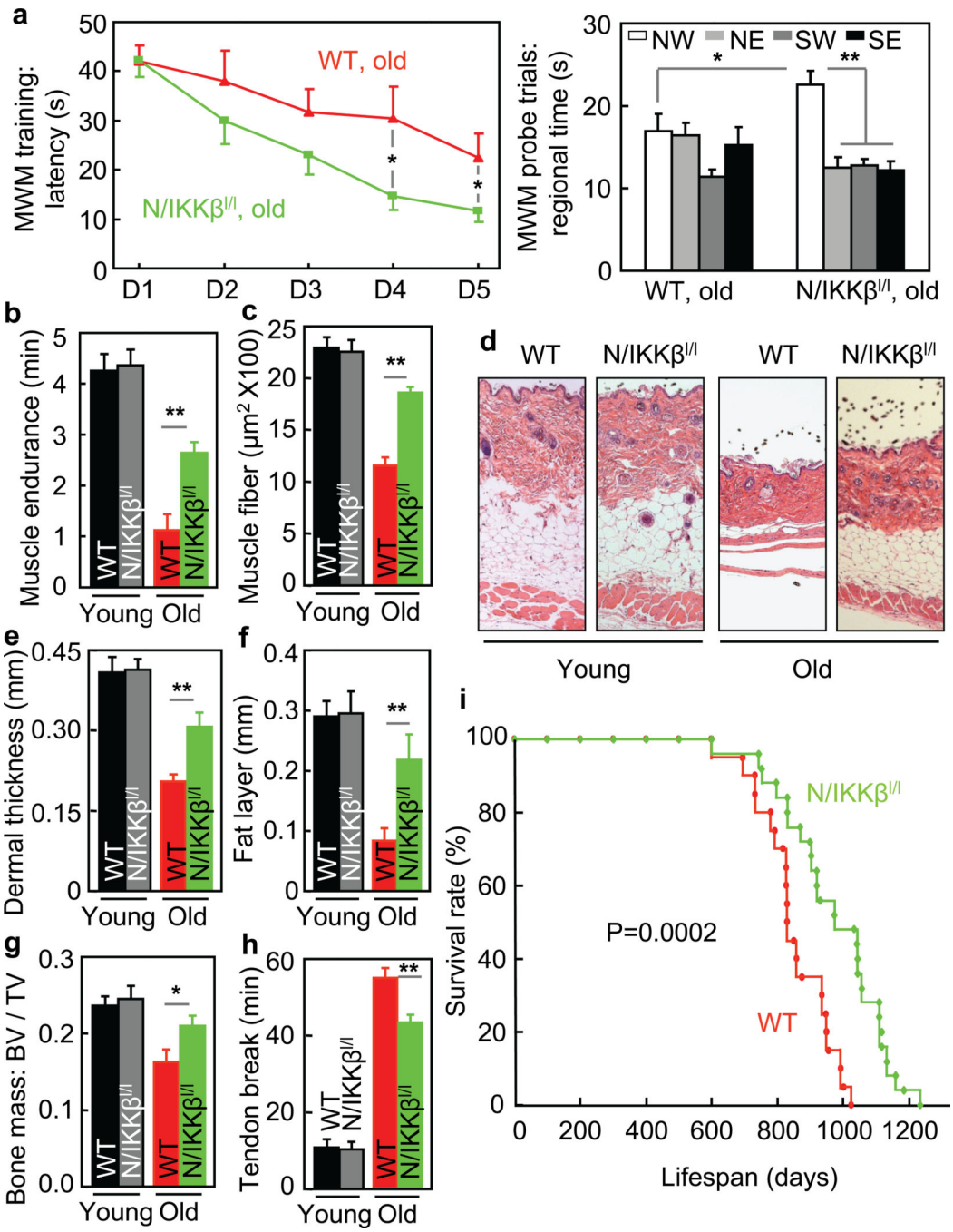

Figure 4. Genetic longevity by brain-specific IKKβ knockout

N/IKKβ$^{lox/lox}$ mice (N/IKKβ$^{l/l}$) and littermate WT in males were maintained on a chow since weaning. **a&b**. Young (3 months) vs. old age (18–20 months) mice were tested for cognition **(a)** and muscle endurance **(b)**. MWM data included time in target northwest (NW) vs. off-target northeast (NE), southwest (SW) and southeast (SE) quadrants in probe trials. **c–h**. Young (3–4 months) vs. old (20–24 months) mice were scarified for assessing muscle (quadriceps) fiber size (**c**), dermal thickness (**d–f**), bone mass (**g**), and tail tendon breaking time (**h**). **i**. Lifespan follow-up (n = 20 in WT and n = 25 in N/IKKβ$^{l/l}$). *P < 0.05, **P <

0.01; young WT: n = 10 **(b)**, 3 **(c&e)**, 5 **(f)**, 6 **(g)** and 8 **(h)**; young N/IKKβ$^{l/l}$: n = 14 **(b)**, 3 **(c,e,f)**, 6 **(g)** and 8 **(h)**; old WT: n = 10 **(a)**, 7 **(b)**, 3 **(c&e)**, 5 **(f&g)**, and 6 **(h);** old N/IKKβ$^{l/l}$ n = 10 **(a)**, 7 **(b)**, 3 **(c,e,f)**, and 6 **(g&h)**. Error bars reflect mean ± SEM.

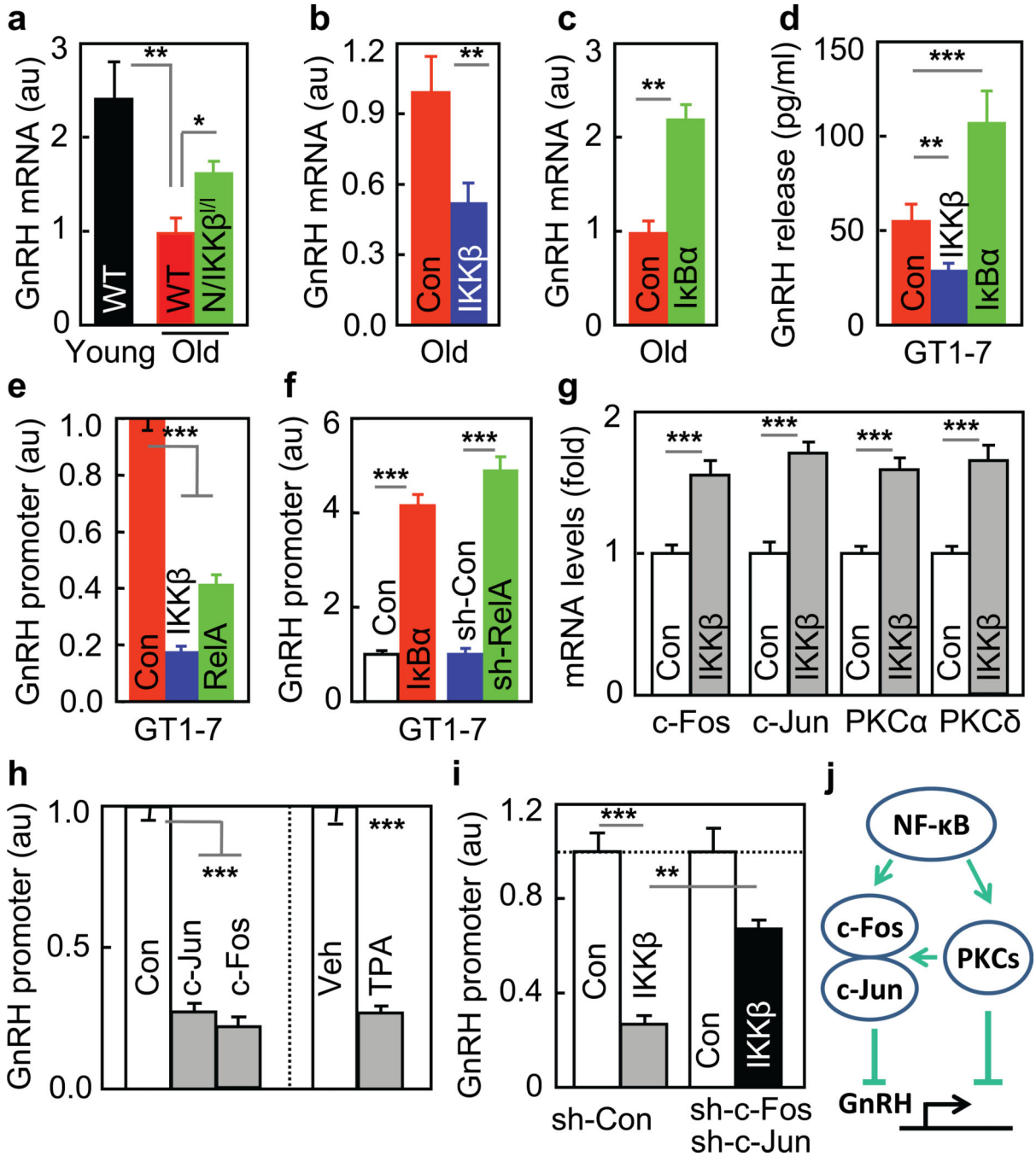

Figure 5. Inhibition of GnRH by IKKβ/NF-κB

a–c Hypothalamic *GnRH* mRNA of indicated mice. **d–g**. GT1–7 cells were transfected with ^{CA}IKKβ, RelA or ^{DN}IκBα vs. control (Con) plasmid **(d,e,g)**, co-transfected with *GnRH*-promoter luciferase plasmid **(e&f)**, or together with *RelA* shRNA (sh-RelA) vs. control shRNA (sh-Con) plasmid **(f)**, and were measure for GnRH release **(d)**, *GnRH* promoter **(e&f)**, and *c-Fos*, *c-Jun*, *PKCα* and *PKCδ* mRNA levels **(g). h**. *GnRH* promoter activities were measured for GT1–7 cells transfected with *GnRH*-promoter luciferase plasmid, co-transfected with *c-Jun* or *c-Fos* plasmid vs. control plasmid (Con), or treated

with TPA vs. vehicle (Veh). **i**. *GnRH* promoter activities were measured for GT1–7 cells transfected with *GnRH*-promoter luciferase plasmid, co-transfected with ^{CA}IKKβ vs. control (Con) plasmid, and with *c-Fos*/c-*Jun* shRNA plasmids (sh-c-Fos/sh-c-Jun) vs. scramble shRNA control (sh-Con). **j**. Summarized schematic model. *P < 0.05, **P < 0.01, ***P < 0.001; n = 12 **(a&e)** and 3 **(f–i)** per group, and n = 6 **(b)**, 8 **(c)** and 4 **(d)** in Con, n = 8 **(b)** and 6 **(d)** in IKKβ, and n = 8 **(c)** and 6 **(d)** in IκBα. Error bars reflect mean ± SEM.

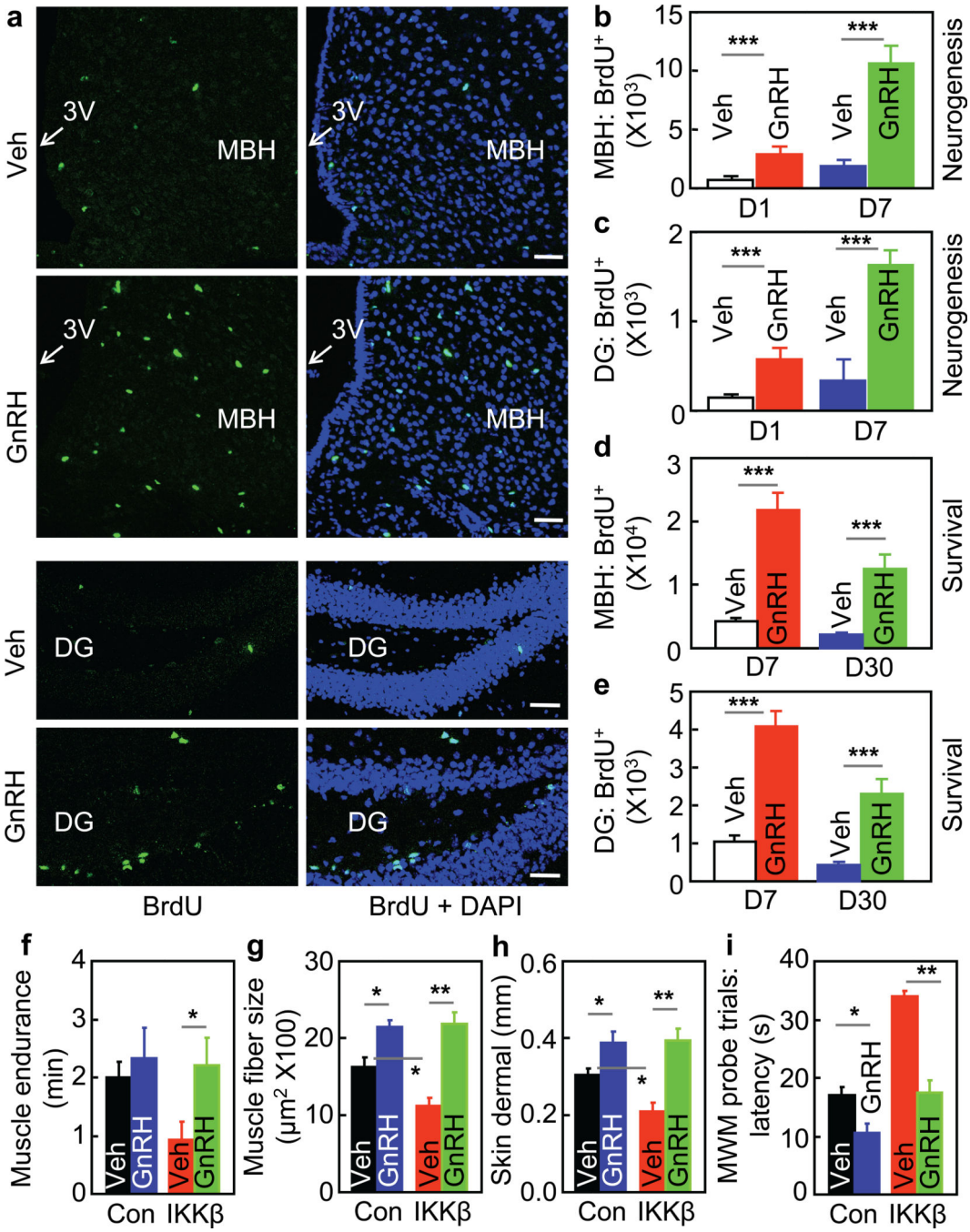

Figure 6. Central and systemic actions of GnRH in counteracting aging

a–d C57BL/6 mice at an old age were subjected to neurogenesis **(a&b)** and survival **(c&d)** assays, as detailed in methods. **a:** BrdU staining of MBH and dentate gyrus (DG) in neurogenesis assay. Bar = 50 μm. **b&c:** BrdU-labeled cells ($BrdU^+$) in the MBH **(b)** and DG **(c)** in neurogenesis assay. **d&e:** Survival of BrdU-labeled ($BrdU^+$) cells in the MBH **(d)** and DG **(e)** in survival assay. **f–i**. MBH-IKKβ and MBH-Con mice at an old age were daily injected subcutaneously with GnRH vs. vehicle for 5 weeks, and analyzed for muscle endurance **(f)**, skeletal muscle fibers**(g)**, skin **(h)**, and cognition **(i)** (see suppl. Fig. 10 for

additional data). *P < 0.05, **P < 0.01, ***P < 0.001; n = 4 **(b–e)**, 7 **(f)**, and 3 **(g&h)** per group, and n = 12 (Con, Veh), 7 (Con, GnRH), 7 (IKKβ, Veh), and 8 (IKKβ, GnRH) **(i)**. Error bars reflect mean ± SEM.